Substantial energy input to the mesopelagic ecosystem from the seasonal mixed-layer pump

Giorgio Dall'Olmo[1,2,3], James Dingle[1], Luca Polimene[1], Robert J.W. Brewin[1,2], Hervé Claustre[4]

[1] *Plymouth Marine Laboratory, UK*

[2] *National Centre for Earth Observations, Plymouth Marine Laboratory, UK*

[3] *Hjort Centre for Marine Ecosystem Dynamics, Bergen, Norway*

[4] *Sorbonne Universités, UPMC Université Paris 06, UMR 7093, Laboratoire d'Océanographie de Villefranche, 06230 Villefranche-sur-Mer, France*

The "mesopelagic" is the region of the ocean between about 100 and 1000 m that harbours one of the largest ecosystems and fish stocks on the planet[1,2]. This vastly unexplored ecosystem is believed to be mostly sustained by chemical energy, in the form of fast-sinking particulate organic carbon, supplied by the biological carbon pump[3]. Yet, this supply appears insufficient to match mesopelagic metabolic demands[4-6]. The mixed-layer pump is a physically-driven biogeochemical process[7-11] that could further contribute to meet these energetic requirements. However, little is known about the magnitude and spatial distribution of this process at the global scale. Here we show that the mixed-layer pump supplies an important seasonal flux of organic carbon to the mesopelagic. By combining mixed-layer depths from Argo floats with satellite retrievals of particulate organic carbon, we estimate that this pump exports a global flux of about 0.3 Pg C

yr^{-1} (range 0.1 – 0.5 Pg C yr^{-1}). In high-latitude regions where mixed-layers are deep, this flux is on average 23%, but can be greater than 100% of the carbon supplied by fast sinking particles. Our results imply that a relatively large flux of organic carbon is missing from current energy budgets of the mesopelagic.

The mesopelagic ecosystem is found below the upper euphotic layer of the ocean where solar radiation is so scarce that photosynthesis stops. The heterotrophic organisms inhabiting this twilight region must therefore depend on other sources of energy. The majority of the mesopelagic energetic requirement is believed to be supplied by organic carbon exported from the surface by the biological pump[1,3-6]. This transfer implicates multiple physical[12-14] and biological[15,16] mechanisms, but gravitational sinking of relatively large particles and aggregates is considered the main force driving this pump[3,15].

One overlooked process that could contribute to the biological carbon pump by supplying additional energy to the mesopelagic is the "mixed-layer pump[10]". This pump is the mechanisms through which carbon is exported below the euphotic zone due to variations in the depth of the surface mixed-layer[7-9]. In essence, organic matter produced at the ocean surface is first transferred to depth by deep mixing and later isolated there by the formation of a new shallower mixed layer. This succession of deep and shallow mixed layers is the critical force that “pumps” carbon to depth. Because fast gravitational sinking rates are not required, the mixed-layer pump can export neutrally-buoyant and slowly-sinking particulate as well as dissolved organic carbon[12,13], that otherwise would not reach the mesopelagic zone.

The organic carbon exported by the mixed-layer pump to the mesopelagic may be either sequestered for climate-relevant time scales, or quickly remineralised and re-exchanged with the atmosphere. Indeed, the fate of the carbon exported by the mixed-layer pump depends on multiple poorly-constrained processes. Small, slowly-sinking particles may be remineralised by the heterotrophic community during the summer and the resulting CO_2 re-ventilated back to the atmosphere by the following winter mixed layer. Under this scenario, the mixed-layer export would not contribute to long-term carbon sequestration. On the other hand, the mixed-layer pump could also sequester carbon for extended periods of time, if the slowly-sinking particles sank below the depth of the following winter mixed layer[12,17]. Regardless of its significance for long-term carbon sequestration, the mixed-layer pump may supply a large fraction of the energy required by the mesopelagic heterotrophic community and thus be an important component of the biological carbon pump.

While the mixed-layer pump can occur on a variety of time scales[7-11], we focus on the *seasonal* mixed-layer pump, which exports organic matter accumulated during the previous summer or produced during the spring, when mixed layers are the deepest and the water column is the least stable (Figure 1). During this spring period, brief stratification events can occur (e.g. due to changes in the sign of the heat flux) and generate conditions favourable for accumulation of fresh phytoplankton biomass[8]. Because the water column is unstable, this stratification can be easily disrupted by the passage of storms[8,19-21] and the accumulated organic matter mixed deeper into the water column. Thus, in the early spring, deep mixed layers can hold significant stocks of organic carbon[12]. Eventually, summer stratification is established by the formation of a stable shallow mixed layer and the organic carbon mixed to depth remains isolated from the surface, generating a seasonal export flux (Figure 1). Few regional studies recognised that significant fluxes of organic matter may be exported by the mixed-layer pump[8,11,18,22]. However, its role in sustaining global mesopelagic ecosystems remains to date unknown.

We combined satellite-estimates of particulate organic carbon (POC, see Supplementary materials) concentration with estimates of the mixed-layer depth (z_m) obtained from the Argo array to quantify POC stocks in the mixed layer. To assess the magnitude of the seasonal mixed-layer pump, we focused on the transition from the time of the maximum winter mixed layer (t_{max}) to the time when summer stratification is established (t_{strat}). During this period, progressively shallower mixed layers form which eventually isolate part of the POC stock below the surface. The mesopelagic is typically defined as the layer of the ocean below the euphotic zone[23]. However, to simplify the calculations, we conservatively estimated the magnitude of the seasonal mixed-layer pump (E_{tot}) as the POC stock isolated below 100 m due to variations of the mixed layer that take place between t_{max} and t_{strat}. This nominal depth-threshold of 100 m is also commonly used in satellite and model estimates of export flux by the biological carbon pump[14,24-26]. We also accounted for the POC accumulated during the previous summer below the mixed-layer before the deepest mixed layer is reached (see Methods). We did not attempt to quantify stocks of fresh dissolved organic carbon (DOC) produced in the spring, because DOC is not readily estimated from satellite data. Finally, we used the relationship between E_{tot} and the depth of the winter mixed layer (z_{max}) to quantify the climatological magnitude and distribution of E_{tot} in the global ocean.

The magnitude and spatial variability of the mixed-layer pump depends strongly on the depth of the winter mixed layer (Figures 2 and S1), with its largest values found at high latitudes in the North Atlantic, Southern Ocean and north-west Pacific. The spatially-integrated climatological estimate of the magnitude of the seasonal mixed-layer pump amounts to approximately 0.26 Pg C yr^{-1} (range 0.10 and 0.53 Pg C yr^{-1}). Therefore, the seasonal mixed-layer pump is responsible for a flux of carbon that is on average 4% (range 2% – 6%) of the currently estimated global carbon export[25-26]. These estimates are conservative, because they do not include the contribution of DOC and because they are derived from a climatological value of z_{max}, which can be significantly smaller than values recorded in individual years.

In high-latitude areas where deep winter mixed layers are common, the proportion of carbon flux by the mixed-layer pump with respect to current estimates of the biological pump can be significant (Figure 3). In these regions, this proportion is on average 23% (mean of the ratios presented in Figure 3 at latitudes >35°N and <35°S), but it can increase to more than 100%. Our findings are in agreement with previous in-situ nutrient budgets[11,18,22] reporting that in regions of the North Atlantic the new production (i.e., a proxy for export[27]) generated before the summer stratification equals the new production taking place during the spring bloom (i.e., after the stratification is established). Collectively, these results demonstrate that in high-latitude regions the mixed-layer pump supplies a major flux of organic carbon to the mesopelagic.

Most methods for measuring carbon export detect the carbon flux generated by particles that sink at relatively fast rates, but do not measure the redistribution of neutrally-buoyant or slowly-sinking organic matter in the water column (see Supplementary materials). Thus, it is unlikely that current global estimates of carbon export include the contribution of the seasonal mixed-layer pump. Our new global estimates should thus be considered as an additional flux of organic carbon to the mesopelagic region that was previously not accounted for.

The mesopelagic ocean is one of the least explored places on the planet and this is especially true in the very productive, but remote and often inaccessible high-latitude regions. Yet, in these regions the interaction between physical, chemical and biological processes sustains vast fisheries, affects the global cycling of chemical elements, and contributes to regulating the Earth's climate[1,28]. Here, we have synergistically exploited satellite and in-situ observations to quantify a poorly-described mechanism that depends on a high-frequency interaction between physical (ephemeral shallow mixed layer formation) and biogeochemical (accumulation of particulate organic carbon) processes. These high-frequency interactions are the most difficult to observe, yet we have found that one of these interactions contributes a major flux of energy to deep ecosystems. New methods are needed to continue filling this observational gap and the growing array of autonomous Biogeochemical-Argo floats[29,30] promises further insights into how the hidden mesopelagic ocean functions.

References

1. Herndl, G. J. and Reinthaler, T. Microbial control of the dark end of the biological pump. *Nature Geosci.* **6,** 718-724 (2013).

2. Irigoien, X. et al. Large mesopelagic fishes biomass and trophic efficiency in the open ocean *Nat. Commun.***5,** 3271 (2014).

3. Volk, T. and Hoffert, M. I. Ocean Carbon Pumps: Analysis of Relative Strengths and Efficiencies in Ocean-Driven Atmospheric CO_2 Changes In *The Carbon Cycle and Atmospheric* CO_2*: Natural Variations Archean to Present*, 99–110 (American Geophysical Union, Washington, D. C., USA, 1985).

4. Burd, A. et al. Assessing the apparent imbalance between geochemical and biochemical indicators of meso- and bathypelagic biological activity: What the @$#! is wrong with present calculations of carbon budgets? *Deep-sea Res. Pt. II* **57,** 1557-1571 (2010).

5. Reinthaler, T. and van Aken, H. M. and Herndl, G. J. Major contribution of autotrophy to microbial carbon cycling in the deep North Atlantic's interior. *Deep-sea Res. Pt. II* **57,** 1572-1580 (2010).

6. Giering, S. L. C. et al. Reconciliation of the carbon budget in the ocean's twilight zone *Nature* **507,** 480 (2014).

7. Woods, J. D. and Onken, R. Diurnal-variation and primary production in the ocean - Preliminary-results of a lagrangian ensemble model. *J. Plankton Res.* **4,** 735-756 (1982).

8. Bishop, J. K. B. and Conte, M. H. And Wiebe, P. H. And Roman, M. R. And Langdon, C. Particulate matter production and consumption in deep mixed layers -

observations in a warm-core ring. *Deep-sea Res. Pt. A* **33,** 1813-1841 (1986).

9. Ho, C. and Marra, J. Early-spring export of phytoplankton production in the northeast Atlantic-ocean. *Mar. Ecol. Prog. Ser.* **114,** 197-202 (1994).

10. Gardner, W. D. and Chung, S. P. and Richardson, M. J. and Walsh, I. D. The oceanic mixed-layer pump. *Deep-sea Res. Pt. II* **42,** 757-775 (1995).

11. Koeve, W. Wintertime nutrients in the North Atlantic - New approaches and implications for new production estimates. *Mar. Chem.* **74,** 245-260 (2001).

12. Dall'Olmo, G. and Mork, K. A. Carbon export by small particles in the Norwegian Sea *Geophys. Res. Lett.* **41,** 2921-2927 (2014).

13. Carlson, C. A. And Ducklow, H. W. And Michaels, A. F. Annual flux of dissolved organic-carbon from the euphotic zone in the northwestern Sargasso sea. *Nature* **371,** 405-408 (1994).

14. Omand, M. M. et al. Eddy-driven subduction exports particulate organic carbon from the spring bloom. *Science* **348,** 222-225 (2015).

15. Buesseler, K. O. et al. Revisiting carbon flux through the ocean's twilight zone. *Science* **316,** 567-570 (2007).

16. Steinberg, D. K. et al. Zooplankton vertical migration and the active transport of dissolved organic and inorganic carbon in the Sargasso Sea. *Deep-sea Res. Pt. I* **47,** 137-158 (2000).

17. Durkin, C. A. and Estapa, M. L. and Buesseler, K. O. Observations of carbon export by small sinking particles in the upper mesopelagic. *Mar. Chem.* **175,** 72-81 (2015).

18. Körtzinger, A. et al. The seasonal pCO(2) cycle at 49 degrees N/16.5 degrees W in the northeastern Atlantic Ocean and what it tells us about biological productivity. *J. Geophys. Res.Oceans* **113,** 1-15 (2008).

19. Koeve, W. and Pollehne, F. and Oschlies, A. and Zeitzschel, B. Storm-induced convective export of organic matter during spring in the northeast Atlantic Ocean. *Deep-sea Res. Pt. I* **49,** 1431-1444 (2002).

20. Waniek, Joanna J. The role of physical forcing in initiation of spring blooms in the northeast Atlantic. *J. Marine Syst.* **39,** 57-82 (2003).

21. Bernardello, R. et al. Factors controlling interannual variability of vertical organic matter export and phytoplankton bloom dynamics - a numerical case-study for the NW Mediterranean Sea *Biogeosciences* **9,** 4233-4245 (2012).

22. Garside, C. and Garside, J. C. The f-ratio on 20-degrees-w during the north-Atlantic bloom experiment. *Deep-sea Res. Pt. II* **40,** 75-90 (1993).

23. Buesseler, K. O. and Boyd, P. W. Shedding light on processes that control particle export and flux attenuation in the twilight zone of the open oceans. *Limnol. Oceanogr.* **54,** 1210-1232 (2009).

24. Henson, S. A. and Sanders, R. and Madsen, E. and Morris, P. J. and Le Moigne, F. and Quartly, G. D. A reduced estimate of the strength of the ocean's biological carbon pump. *Geophys. Res. Lett.* **38,** L04606 (2011).

25. Cabre, A. and Marinov, I. and Leung, S. Consistent global responses of marine ecosystems to future climate change across the IPCC AR5 earth system models. *Clim. Dynam.* **45,** 1253-1280 (2015).

26. Siegel, D. A. et al. Global assessment of ocean carbon export by combining satellite

observations and food-web models. *Global Biogeochem. Cy.* **28,** 2013GB004743 (2014).

27. Eppley, R. W. and Peterson, B. J. Particulate organic matter flux and planktonic new production in the deep ocean. *Nature* **282,** 677-680 (1979)

28. Kwon, E. Y. and Primeau, F. and Sarmiento, J. L. The impact of remineralization depth on the air-sea carbon balance. *Nature Geosci.* **2,** 630-635 (2009).

29. Claustre, H. et al. Bio-optical Profiling Floats as New Observational Tools for Biogeochemical and Ecosystem Studies: Potential Synergies With Ocean Color Remote Sensing. In *Proceedings of OceanObs'09: Sustained Ocean Observations and Information for Society (Vol. 2)* (European Space Agency, Venice, Italy, 2010).

30. Biogeochemical Argo Task Team. 2016. *The rationale, design and implementation plan for Biogeochemical Argo* (http://www3.mbari.org/chemsensor/BGCArgoPlanJune21.pdf)

139

Acknowledgements Temperature and salinity data were collected and made freely available by the International Argo Program and the national programs that contribute to it (http://www.argo.ucsd.edu, http://argo.jcommops.org). The Argo Program is part of the Global Ocean Observing System. For their roles in producing, coordinating, and making available the CMIP5 model output, we acknowledge the climate modelling groups at NOAA-GFDL and at the UK MetOffice Hadley Centre, the World Climate Research Programme's (WCRP) Working Group on Coupled Modelling (WGCM), and the Global Organization for Earth System Science Portals (GO-ESSP). M.J. Behrenfeld is thanked for providing insightful comments on a first draft of this manuscript. D. Siegel and S. Henson are thanked for providing their results used for preparing Figure 3. R. Dall'Olmo is acknowledged for help in preparing Figure 1. G.D.O. and R.B. acknowledge funding from the UK National Centre for Earth Observation and Marie Curie FP7-PIRG08-GA-2010-276812. L.P. was funded through (UK) NERC National Capability in Sustained Observations and Marine Modelling. H.C. acknowledges funding from the European Research Council for the remOcean project (GA 246777). Earth Observation data were supplied by the NERC EO Data Acquisition and Analysis Service. This work is a contribution to the Ocean Colour Climate Change Initiative of the European Space Agency.

Correspondence Correspondence and requests for materials should be addressed to G.D.O. (email: gdal@pml.ac.uk).

Author contributions: G.D.O. designed the study. G.D.O. and J.D. conducted the data analysis. G.D.O., L.P., R.J.B. interpreted the results and wrote the manuscript. H.C. provided Bio-Argo data. All authors commented on the manuscript.

Competing financial interests The authors declare that they have no competing

financial interests.

Figure captions

Figure 1. Schematic representation of the seasonal mixed-layer pump. In the spring the depth of the mixed layer (yellow line) reaches its maximum annual value. Before and during this event, ephemeral stratification events can occur due, for example, to intermittent changes in the heat flux from negative (out of the ocean, blue arrows) to positive (into the ocean, red arrows). These stratification events can result in new accumulation of organic matter, which is then re-distributed over the water column by subsequent deep mixing. Eventually, when the summer stratification is established, the deeply-mixed organic matter remains isolated below the sunlit layer, resulting in an export of carbon. Orange, white and green squares and circles represent small particles accumulated within and below the surface mixed layer during the previous summer and produced due to the ephemeral stratification events, respectively.

Figure 2. Relationship between winter mixed layer depth and export by the mixed-layer pump. (a) climatological deepest winter mixed layers (z_{max}, black colours refer to regions with z_{max}<100 m and not considered in this study) and (b) estimates of particulate carbon export by the mixed-layer pump (E_{tot}).

Figure 3. Comparison between mixed-layer pump and biological pump. Ratio of carbon exported by the mixed-layer pump and estimates of the biological carbon pump by satellite-based algorithms: (a) E_{tot}:TotEZ for reference 26, (b) E_{tot}:H11 for reference 24); and by two Earth System Models (c) GFDL-ESM2M and (d) HadGEM2-ES. Regions with ratios greater than 1 indicate our estimates of carbon export by the mixed-layer carbon pump are higher than current estimates of the biological pump. Black colours refer to regions with z_{max}<100 m and not considered in this study.

Methods

Ocean Colour Data and POC estimates. Surface POC (mg m^{-3}) was estimated from remote-sensing reflectance data (8-day temporal and 4-km spatial resolution) generated by the European Space Agency Ocean Colour Climate Change Initiative (ESA OC-CCI) project[31] using the standard NASA remote-sensing algorithm based on the reflectance ratio at 490 and 555 nm[32]. To compute POC at latitudes south of 35°S we used a Southern Ocean regional algorithm based on the reflectance ratio at 443 and 555 nm[33]. Frequency distributions of the POC values estimated at the time of the deepest mixed layer and of stratification are presented in Figure S2.

Argo data and mixed-layer estimates. The global Argo dataset was filtered to remove floats that did not meet the following criteria: a) profiles were collected for at least 365 days; b) all profiles had coincident measurements of temperature, salinity and pressure; c) all pressure data increased monotonically between >0 and <2100 dbars; d) all temperature data were >−10 and <+50°C; e) all salinity data were >0 and <45 psu. Using only the floats that passed the filtering procedure, the depth of the mixed layer, z_m (m), was derived using a density-based algorithm[34]. The analysis is based on all satellite data collected between 1997 and 2012 and all Argo profiles that passed the above filtering procedure. Nevertheless, due to increased number of satellite data points and of Argo profiles available from the year 2002 onwards, the results presented below are mostly based on data from the years 2006-2011 (Figure S3).

POC flux generated by the seasonal mixed-layer pump. To compute the carbon flux generated by the seasonal mixed-layer pump, the following procedure was applied to each float dataset that contained profiles for a minimum of 320 days:

1. The time (t_{max}) and value (z_{max}) of the deepest z_m were identified.

2. A timeseries of z_m was extracted starting at t_{max} and conservatively ending 9 months after z_{max}. Only timeseries without missing data were selected. Timeseries without missing data were defined as those timeseries for which the maximum time interval between profiles did not exceed 5 times the modal time step between all profiles.

3. The beginning of the summer stratification was estimated based on a criterion developed to account for the inherent geographic variability of z_{max}. First, to ensure that the transition to the summer stratification had begun, the "time of mid-shoaling" was identified as the time after t_{max} when z_m reached a value that was half of the range of z_m during the timeseries. Then, from the part of the timeseries following the mid-shoaling, the time t_{strat} was extracted after which z_m did not vary by more than 20% of z_{max} per 10-day period for at least 30 days. The time between t_{max} and t_{strat} is indicated as Δt.

4. For each profile between t_{max} and t_{strat}, the average surface POC was then extracted from a grid of 8 × 8 satellite pixels centred on the location of and closest in time to the profile. Only years for which all POC and z_m values were available during Δt were used.

5. We assumed that the POC concentration is homogeneous in the mixed layer (optical backscattering data from Bio-Argo floats have been used to verify this hypothesis, see Supplementary materials and Figure S4). The POC stock in the mixed layer for each profile was then computed as the product of the POC concentration at the surface and the depth of the mixed layer.

6. The variation in the POC stock isolated below the mixed layer between times t_{i-1} and t_i was estimated as:

$$E(t_i) = \begin{cases} +POC(t_{i-1})[z_m(t_{i-1}) - z_m(t_i)], & if\ z_m(t_i) \leq z_m(t_{i-1}) \\ -POC(t_{i-2})[z_m(t_i) - z_m(t_{i-1})], & if\ z_m(t_i) > z_m(t_{i-1}) \end{cases} \quad (1)$$

where the formulation for $z_m(t_i) \leq z_m(t_{i-1})$ was used to compute the increase in the POC isolated below the mixed layer at time t_i due to a shoaling of the mixed layer, while the formulation for $z_m(t_i) > z_m(t_{i-1})$ was used to compute a decrease of the POC isolated below the mixed layer due to re-entrainment after a temporary deepening of the mixed layer.

7. The POC exported by the mixed-layer pump at the time of stratification was finally estimated as the sum of POC stock variations below 100 m during all time steps between the time of the deepest mixed layer and the time of stratification, multiplied by the fraction (*1-B*) of this carbon stock that is not due to POC present in the mesopelagic before the deepening of the mixed layer (see below the explanation for how *B* was estimated):

$$E_{tot} = (1 - B) \sum_{t_{max+1}}^{t_{strat}} E\,(t_i). \quad (2)$$

The nominal depth of 100 m was chosen as the depth where the upper sunlit ocean layer ends and where the mesopelagic zone begins. This is a common threshold for the upper boundary of the mesopelagic[6], and for the bottom of the euphotic zone, especially in high-latitude regions[26]. This depth is also consistent with other studies estimating carbon export (e.g., IPCC CMIP5 models[25], as well as current satellite estimates[24,26]).

E_{tot} parametrization based on z_{max}. In order to provide a parametrization for E_{tot}, a regression analysis was carried out between E_{tot} values and their corresponding values of z_{max}. The bootstrap method (with 1000 simulated samples) was employed to estimate the coefficients of this relationship and their uncertainties (Figure S5). This relationship was then applied to climatological gridded winter mixed-layer depths obtained from the publicly available z_m product[34] to obtain a global estimation of the E_{tot} at a 1-degree resolution.

Uncertainty estimates / Sensitivity analysis. A sensitivity analysis was carried out to estimate a plausible range of uncertainties associated with our E_{tot} values. Specifically, we investigated how the derived values of E_{tot} are affected by the following uncertainties: uncertainty in POC, z_m and the definition of t_{strat}. Uncertainties for each of these variables are presented in Supplementary Table 1. Results of this analysis are reported as the median value of the ratio of the nominal values of E_{tot} calculated for each year and each float to the values of E_{tot} computed when each parameter was varied separately. These results demonstrate that E_{tot} is mostly sensitive to uncertainties in POC and z_m.

Duration of the transition between z_{max} and z_{strat}. One of the parameters determining the value of E_{tot} is the duration of the transition between the timing of the deepest mixed layer and of stratification (i.e., Δt). Figure S6 demonstrates that this transition is rapid, with a median value of 20 days and 80% of the shoaling events occurring 40 days after the deepest mixed layer.

Estimating the mesopelagic background stocks of POC. When mixed layers at the end of the summer start deepening and begin transferring surface particles deeper into the mesopelagic region, other particles may be already present below the mixed layer. As a consequence, as mixed layers deepen, they not only transfer surface particles to depth, but they also re-entrain existing mesopelagic particles. Therefore, to accurately estimate the stock of carbon that is transferred to the mesopelagic by the mixed layer pump, it is necessary to remove the contribution of these background particles already present below the mixed layer from the signals recorded by satellite sensors at the surface.

Because ocean-colour satellites only sense the upper part of the water column, to estimate this contribution we employed a data set collected by Biogeochemical-Argo floats. These floats were mostly deployed in regions with deep mixed layers and mounted optical sensors that can be used to determine particulate backscattering (b_{bp}), which is a proxy of POC (e.g., reference 10). We then computed the fraction B=E_{bck}:E_{tot} of background POC stock (E_{bck}) to E_{tot} as follows. We extracted each year of data from each float and computed E_{tot} using the same methodology employed for the core-Argo floats and satellite data employed for the main analysis. However, instead of satellite estimates of POC, we used estimates of POC derived from the float b_{bp} data in the mixed layer. For each year of data and each float, we then computed the average background POC concentration below the mixed layer and above z_{max} during the three months preceding t_{max}. The average stock of background POC present between 100 m and z_{max} (E_{bck}) was computed by multiplying this average concentration of background POC by the depth difference ($z_{max} - 100$). The bio-optical model used to convert b_{bp} into POC is a simple multiplicative factor[10], thus the resulting values of B are independent of the conversion factor.

The average yearly locations and estimates of B for all floats are presented in Figure S7. A total of 59 independent estimates were obtained, once data were filtered to only include years where z_{max}>150m. Overall, the median B value was 0.51±0.18, where the uncertainty range was computed as half the range between the 84th and 16th

percentile, which corresponds to one standard deviation if the distribution is normal. We also tested the sensitivity of this result to the length of the period before z_{max} over which the background is computed. We found that by varying this parameters by ±2 months with respect to the nominal value of 3 months, B changed by less than 10%, supporting the robustness of this result.

Comparison with carbon export by the biological carbon pump estimated by Earth System Models. We compared our estimates of E_{tot} to estimates of the sinking particulate carbon export flux at 100 m from two representative[25] Coupled Model Intercomparison Project Phase 5 (CMIP5) models with explicit marine ecological modules. We used the "historic" yearly simulation for the year 2005 from the US NOAA GFDL-ESM2M[35] and UK MetOffice HadGEM2-ES[36].

Data availability. The satellite ocean-colour data used in the analysis are available from the ESA OC-CCI website (http://www.esa-oceancolour-cci.org). Argo data are available from the official Argo web site (http://www.argodatamgt.org/Documentation/Access-via-FTP-on-GDAC). Climatological gridded winter mixed-layer depths can be obtained from http://mixedlayer.ucsd.edu. The US NOAA GFDL-ESM2M and UK MetOffice HadGEM2-ES datasets are made available by the UK Centre for Environmental Data Archival (http://www.ceda.ac.uk). Data from Bio-Argo floats are available from the Coriolis data centre (http://www.argodatamgt.org/Documentation/Access-via-FTP-on-GDAC) and from the Monterey Bay Aquarium Research Institute website (http://www.mbari.org/science/upper-ocean-systems/chemical-sensor-group/floatviz).

References cited in Methods

31. Brewin, R. J. W. et al. The Ocean Colour Climate Change Initiative: III. A round-robin comparison on in-water bio-optical algorithms. *Remote Sens. Environ.* **162,** 271-294 (2015).

32. Stramski, D. et al. Relationships between the surface concentration of particulate organic carbon and optical properties in the eastern South Pacific and eastern Atlantic Oceans. *Biogeosciences* **5,** 171-201 (2008).

33. Allison, D. B. and Stramski, D. and Mitchell, B. G. Empirical ocean color algorithms for estimating particulate organic carbon in the Southern Ocean. *J. Geophys. Res.* **115,** C10044 (2010).

34. Holte, J. and Talley, L. A new algorithm for finding mixed layer depths with applications to Argo data and Subantarctic Mode Water formation. *J. Atmos. Oceanic Technol.* **26,** 1920-1939 (2009).

35. Dunne, J. P. et al. GFDL's ESM2 Global Coupled Climate-Carbon Earth System Models. Part II: Carbon System Formulation and Baseline Simulation Characteristics. *J.Climate* **26,** 2247-2267 (2013).

36. Palmer, J. R. and Totterdell, I. J. Production and export in a global ocean ecosystem model. *Deep-sea Res. Pt. I* **48,** 1169-1198 (2001).

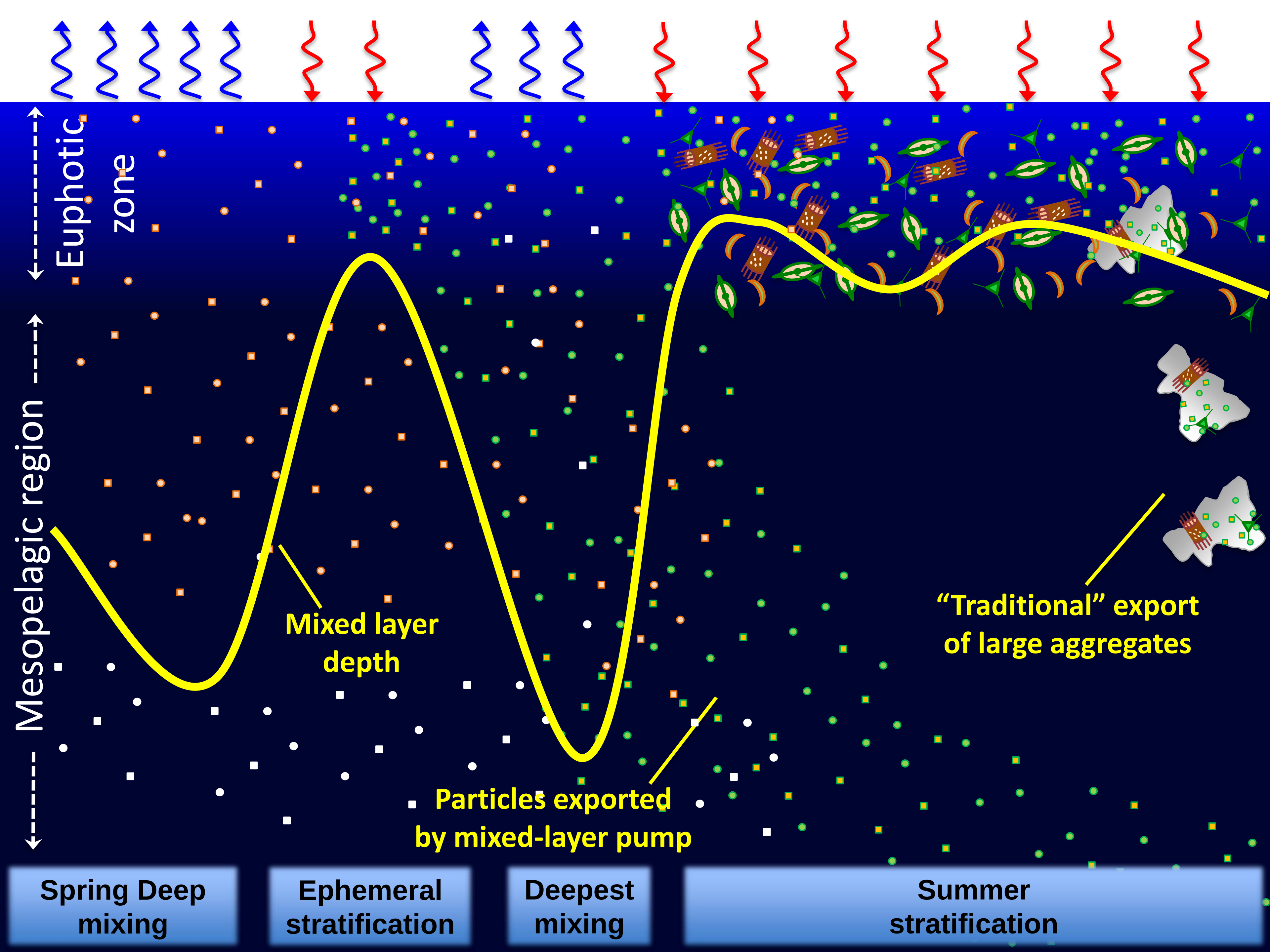
Euphotic zone
Mesopelagic region
Mixed layer depth
"Traditional" export of large aggregates
Particles exported by mixed-layer pump
Spring Deep mixing
Ephemeral stratification
Deepest mixing
Summer stratification

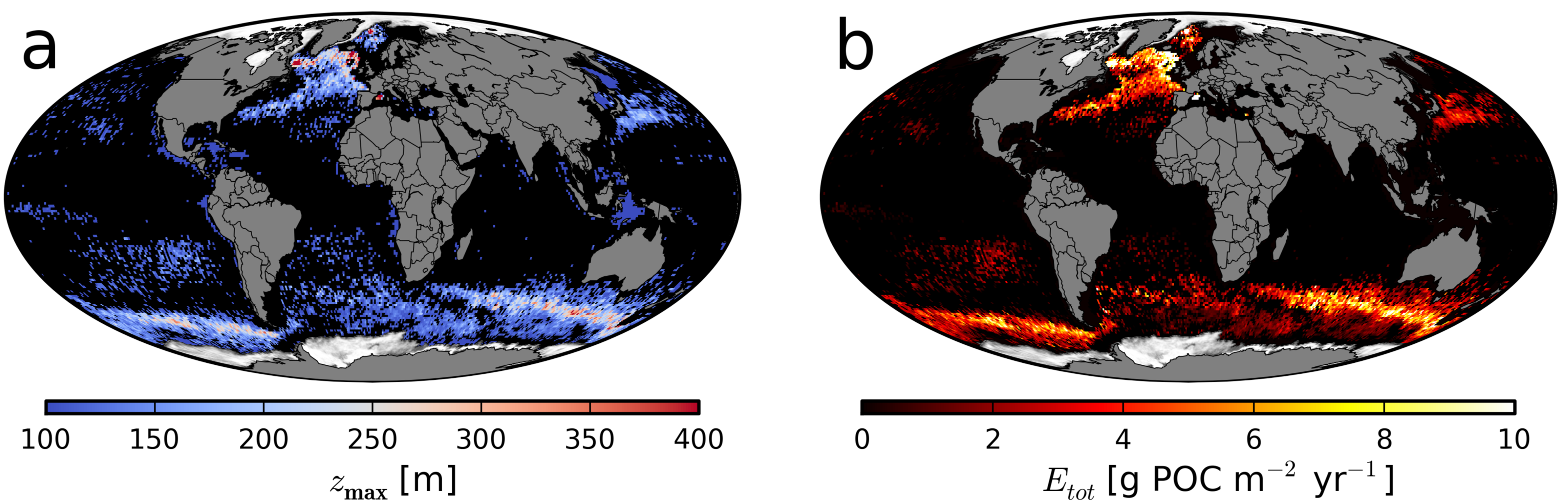

a
100
150
200
250
300
350
400
$z_{\mathbf{max}}$ [m]
b
0
2
4
6
8
10
E_{tot} [g POC m^{-2} yr^{-1}]

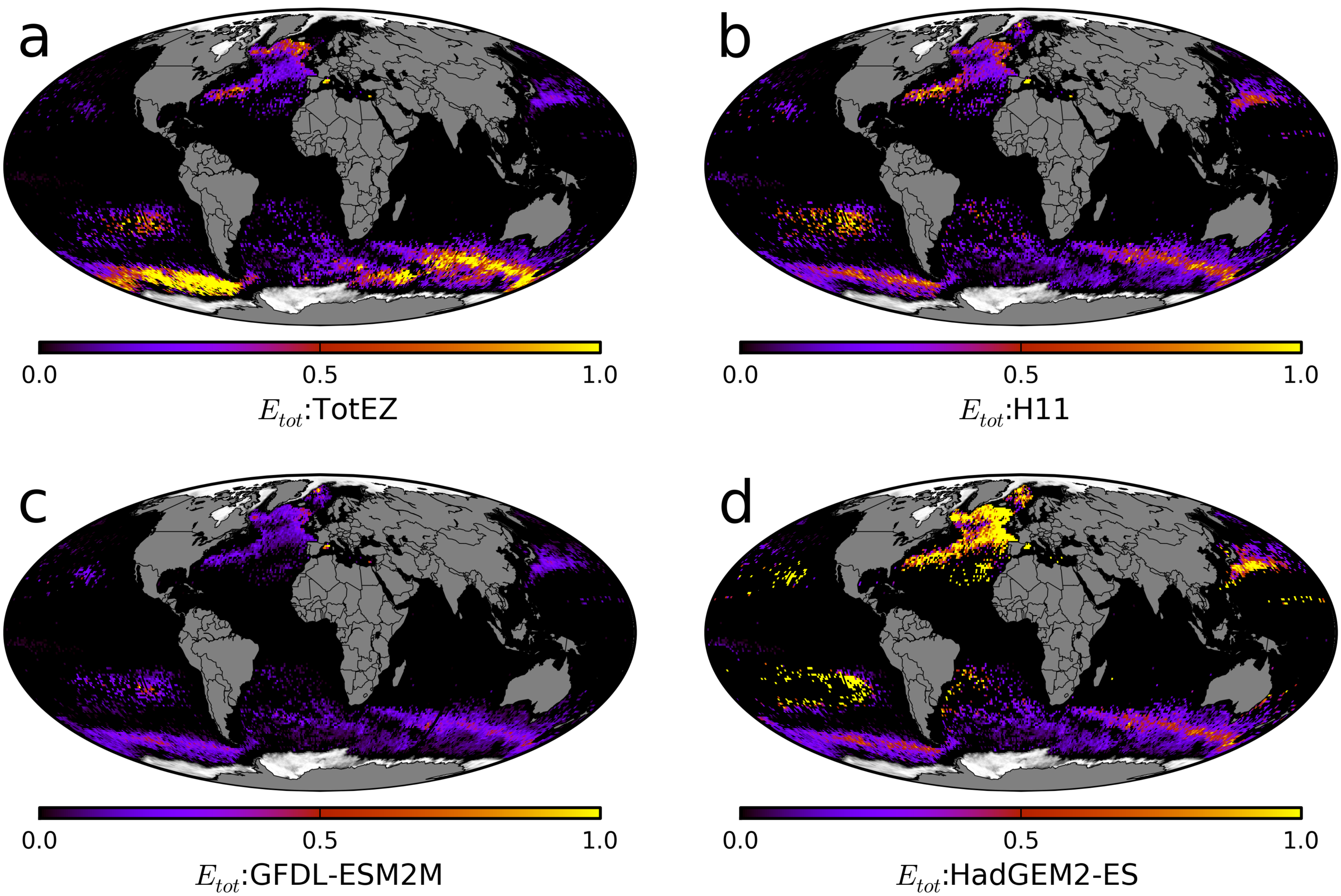
a
0.0
0.5
1.0
E_{tot}:TotEZ
b
0.0
0.5
1.0
E_{tot}:H11
c
0.0
0.5
1.0
E_{tot}:GFDL-ESM2M
d
0.0
0.5
1.0
E_{tot}:HadGEM2-ES